fractal and fractional

Article

Circuit of Quantum Fractional Fourier Transform

Tieyu Zhao [1,*] and Yingying Chi [2]

[1] Information Science Teaching and Research Section, Northeastern University at Qinhuangdao, Qinhuangdao 066004, China
[2] College of Marxism, Northeastern University at Qinhuangdao, Qinhuangdao 066004, China; chiyingying@neuq.edu.cn
* Correspondence: zhaotieyu@neuq.edu.cn

Abstract: In this paper, we first use the quantum Fourier transform (*QFT*) and quantum phase estimation (*QPE*) to realize the quantum fractional Fourier transform (*QFrFT*). As diverse definitions of the discrete fractional Fourier transform (*DFrFT*) exist, the relationship between the *QFrFT* and a classical algorithm is then established; that is, we determine the classical algorithm corresponding to the *QFrFT*. Second, we observe that many definitions of the multi-fractional Fourier transform (*mFrFT*) are flawed: when we attempt to propose a design scheme for the quantum *mFrFT*, we find that there are many invalid weighting terms in the definition of the *mFrFT*. This flaw may have very significant impacts on relevant algorithms for signal processing and image encryption. Finally, we analyze the circuit of the *QFrFT* and the reasons for the observed defects.

Keywords: quantum fractional Fourier transform; quantum Fourier transform; quantum phase estimation; quantum computing

check for updates

Citation: Zhao, T.; Chi, Y. Circuit of Quantum Fractional Fourier Transform. *Fractal Fract.* **2023**, *7*, 743. https://doi.org/10.3390/fractalfract7100743

Academic Editors: Zunwei Fu, Bingzhao Li, Xiangyang Lu and Ahmed Zayed

Received: 24 August 2023
Revised: 28 September 2023
Accepted: 7 October 2023
Published: 8 October 2023

1. Introduction

In recent years, research into and the application of quantum information technology—represented by quantum computing, quantum communication, and quantum measurement—have accelerated globally, with many countries increasing investments and broadening project layouts. Quantum computing is expected to fundamentally improve the speed of information processing, quantum communication will greatly improve communication security, and quantum precision measurement and sensing technology will have extensive applications in the future digital age and the era of the Internet of Things. Quantum computing is a novel computation mode that follows the laws of quantum mechanics to regulate the calculation of quantum information units, utilizing the characteristics of quantum mechanics [1] (e.g., superposition and entangled states) for the storage, processing, and transmission of information. Since Feynman proposed the concept of quantum computing [2], researchers have shown great interest in the high parallelism and speed provided by such an approach. The discovery of Shor's efficient decomposition algorithm [3] aroused interest in the quantum implementation of modular arithmetic operations, which are the basis of quantum decomposition circuits. The core of Shor's algorithm is the quantum Fourier transform (*QFT*) [4]. In the field of quantum computing, involving topics such as quantum information processing [5], quantum machine learning [6], quantum neural networks [7], and so on, a series of significant theoretical improvements and encouraging experimental results have recently been achieved, in which the *QFT* plays an important role. Quantum image processing plays an important role in satisfying the demands of machine vision, and quantum image representation is the basis of quantum image processing. The representation of quantum images has been developed from the initial Qubit Lattice [8], Real Ket [9], and Entangled image [10] to the common representation forms FRQI [11] and NEQR [12]. Based on these characterizations, various methods for quantum image processing have also been proposed [13], such as local feature point extraction of quantum images [14], weighted filtering of quantum images in the spatial domain [15], and restoration of quantum image noise removal [16]. Among them, the *QFT* plays an important role in frequency domain filtering [17,18], and the quantum arithmetic operations associated with the *QFT* are equally important to consider [19]. It is clear that the *QFT* plays an important role in quantum algorithm design and information processing.

As an extended definition of the Fourier transform (*FT*), the fractional Fourier transform (*FrFT*) has become one of the most actively researched subjects in signal processing and has been widely used in optics, image and signal processing, and communication [20–24]. However, at present, there are few studies on the quantum fractional Fourier transform (*QFrFT*) [25–28]. The only existing studies have also been conducted from the perspective of quantum mechanics, in order to study the theory underlying the *QFrFT*, and have not presented circuits for realization of the *QFrFT*. In this paper, the *QFrFT* is designed by means of the *QFT* and quantum phase estimation (*QPE*) [1]. The idea is to retain the eigenvector of the *QFT*, realize the fractional power of the eigenvalue by introducing two phase gates, and finally obtain the *QFrFT* by combining the eigenvalue of the fractional power with the eigenvector.

The remainder of this paper is organized as follows. The *QFrFT* is proposed in Section 2. Section 3 explains the correspondence between the *QFrFT* and a classical algorithm. The flaws of the *mFrFT* are detailed in Section 4. In Section 5, circuits for the *QFrFT* and *mFrFT* are discussed. Finally, the conclusions are presented in Section 6.

2. Quantum Fractional Fourier Transform

At present, some related studies on the *QFrFT* have been proposed [25–28], but these studies have not presented specific quantum circuits. Parasa et al. have even stated that the *QFrFT* is impossible to achieve [25]. In this section, we use the *QFT* and *QPE* to design the *QFrFT*.

For a unitary matrix U, assuming that it has an eigenvector $|u\rangle$ and the corresponding eigenvalue $e^{2\pi i\varphi}$, then $U|u\rangle = e^{2\pi i\varphi}|u\rangle$ is satisfied. Therefore, we can calculate φ through the *QPE*. The circuit is shown in Figure 1. It is not difficult to find that the *QFT* is the key of phase estimation, and phase estimation is the key of many quantum algorithms.

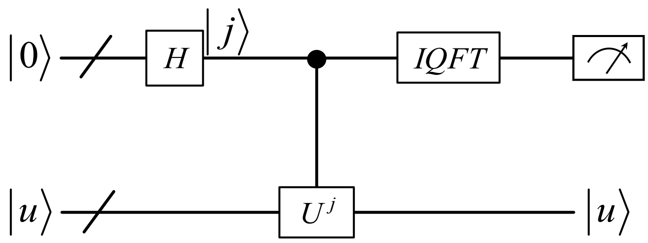

Figure 1. Circuit for quantum phase estimation.

We know the relationship between the eigenvalues and eigenvectors of the discrete Fourier transform (*DFT*), as shown in Equation (1):

$$F|u\rangle = D|u\rangle, \tag{1}$$

where F denotes the Fourier transform, D is the eigenvalue, and $|u\rangle$ is the eigenvector. The discrete fractional Fourier transform (*DFrFT*) has the same eigenvector $|u\rangle$ as the *DFT*, and the correspondence between the eigenvalue and eigenvector is shown in Equation (2):

$$F^{\alpha}|u\rangle = D^{\alpha}|u\rangle, \tag{2}$$

where F^{α} denotes the *FrFT*, and D^{α} is the eigenvalue. Thus, we can determine the eigenvalue of the *QFrFT* by means of the *QPE*, as depicted in Figure 2.

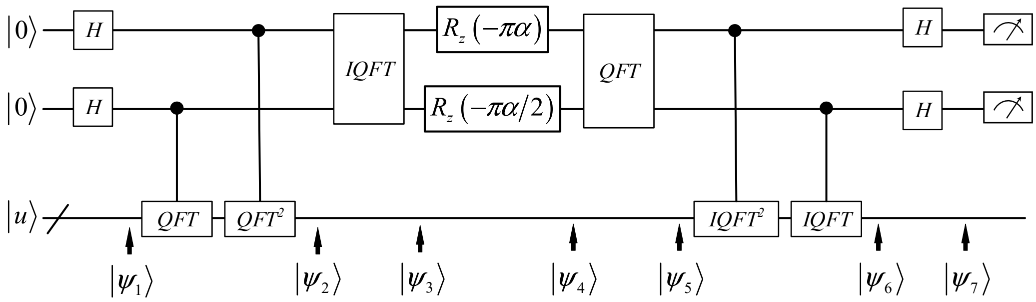

Figure 2. Circuit for the *QFrFT*.

The process is as follows:

$$\begin{aligned}|\psi_1\rangle &= \tfrac{1}{\sqrt{2}}(|0\rangle+|1\rangle)\otimes\tfrac{1}{\sqrt{2}}(|0\rangle+|1\rangle)\otimes|u\rangle \\ &= \tfrac{1}{2}(|00\rangle+|01\rangle+|10\rangle+|11\rangle)\otimes|u\rangle\end{aligned}. \tag{3}$$

Thus, we can obtain

$$|\psi_2\rangle = \frac{1}{2}\Big(|00\rangle I|u\rangle + |01\rangle F|u\rangle + |10\rangle F^2|u\rangle + |11\rangle F^3|u\rangle\Big). \tag{4}$$

Here, $|u\rangle$ is the eigenvector of the *FT*. From Equation (1), we can obtain

$$|\psi_2\rangle = \frac{1}{2}\Big(|00\rangle D^0|u\rangle + |01\rangle D^1|u\rangle + |10\rangle D^2|u\rangle + |11\rangle D^3|u\rangle\Big). \tag{5}$$

The eigenvalue D can be expressed as:

$$D = \begin{pmatrix}\lambda_0 & & & 0\\ & \lambda_1 & & \\ & & \ddots & \\ 0 & & & \lambda_{n-1}\end{pmatrix}, \tag{6}$$

where $\lambda_j \in \{1, i, -1, -i\}$; $j = 0, 1, \cdots, n-1$. The 2-qubit inverse quantum Fourier transform (*IQFT*) is used in the control register, and its matrix can be expressed as:

$$IQFT = \frac{1}{\sqrt{4}}\begin{pmatrix}1 & 1 & 1 & 1\\ 1 & i & -1 & -i\\ 1 & -1 & 1 & -1\\ 1 & -i & -1 & i\end{pmatrix}. \tag{7}$$

After 2-qubit *IQFT*, we obtain

$$|\psi_3\rangle = \frac{1}{4}(Q|00\rangle + W|01\rangle + E|10\rangle + R|11\rangle)\otimes|u\rangle \tag{8}$$

where

$$\begin{cases} Q = D^0 + D^1 + D^2 + D^3\\ W = D^0 + iD^1 - D^2 - iD^3\\ E = D^0 - D^1 + D^2 - D^3\\ R = D^0 - iD^1 - D^2 + iD^3\end{cases}. \tag{9}$$

Moreover, from Equations (6) and (9), we have

$$Q = D^0 + D^1 + D^2 + D^3 = \begin{pmatrix} \lambda_0^0 + \lambda_0^1 + \lambda_0^2 + \lambda_0^3 & & & \\ & \lambda_1^0 + \lambda_1^1 + \lambda_1^2 + \lambda_1^3 & & \\ & & \ddots & \\ & & & \lambda_{n-1}^0 + \lambda_{n-1}^1 + \lambda_{n-1}^2 + \lambda_{n-1}^3 \end{pmatrix}, \quad (10)$$

$$W = D^0 + iD^1 - D^2 - iD^3 = \begin{pmatrix} \lambda_0^0 + i\lambda_0^1 - \lambda_0^2 - i\lambda_0^3 & & & \\ & \lambda_1^0 + i\lambda_1^1 - \lambda_1^2 - i\lambda_1^3 & & \\ & & \ddots & \\ & & & \lambda_{n-1}^0 + i\lambda_{n-1}^1 - \lambda_{n-1}^2 - i\lambda_{n-1}^3 \end{pmatrix}, \quad (11)$$

$$E = D^0 - D^1 + D^2 - D^3 = \begin{pmatrix} \lambda_0^0 - \lambda_0^1 + \lambda_0^2 - \lambda_0^3 & & & \\ & \lambda_1^0 - \lambda_1^1 + \lambda_1^2 - \lambda_1^3 & & \\ & & \ddots & \\ & & & \lambda_{n-1}^0 - \lambda_{n-1}^1 + \lambda_{n-1}^2 - \lambda_{n-1}^3 \end{pmatrix}, \quad (12)$$

and

$$R = D^0 - iD^1 - D^2 + iD^3 = \begin{pmatrix} \lambda_0^0 - i\lambda_0^1 - \lambda_0^2 + i\lambda_0^3 & & & \\ & \lambda_1^0 - i\lambda_1^1 - \lambda_1^2 + i\lambda_1^3 & & \\ & & \ddots & \\ & & & \lambda_{n-1}^0 - i\lambda_{n-1}^1 - \lambda_{n-1}^2 + i\lambda_{n-1}^3 \end{pmatrix}. \quad (13)$$

Here, the eigenvalues are $\lambda_j \in \{1, i, -1, -i\}$; $j = 0, 1, \cdots, n-1$. Thus, Equations (10)–(13) can be written as:

$$Q = \begin{cases} \lambda_j^0 + \lambda_j^1 + \lambda_j^2 + \lambda_j^3 = 4 & if \quad \lambda_j = 1 \\ \lambda_j^0 + \lambda_j^1 + \lambda_j^2 + \lambda_j^3 = 0 & if \quad \lambda_j = i, -1, -i \end{cases}, \quad (14)$$

$$W = \begin{cases} \lambda_j^0 + i\lambda_j^1 - \lambda_j^2 - i\lambda_j^3 = 4 & if \quad \lambda_j = -i \\ \lambda_j^0 + i\lambda_j^1 - \lambda_j^2 - i\lambda_j^3 = 0 & if \quad \lambda_j = 1, i, -1 \end{cases}, \quad (15)$$

$$E = \begin{cases} \lambda_j^0 - \lambda_j^1 + \lambda_j^2 - \lambda_j^3 = 4 & if \quad \lambda_j = -1 \\ \lambda_j^0 - \lambda_j^1 + \lambda_j^2 - \lambda_j^3 = 0 & if \quad \lambda_j = 1, i, -i \end{cases}, \quad (16)$$

and

$$R = \begin{cases} \lambda_j^0 - i\lambda_j^1 - \lambda_j^2 + i\lambda_j^3 = 4 & if \quad \lambda_j = i \\ \lambda_j^0 - i\lambda_j^1 - \lambda_j^2 + i\lambda_j^3 = 0 & if \quad \lambda_j = 1, -1, -i \end{cases}. \quad (17)$$

Then, the eigenvalues of the *FT* are preserved in the quantum state, as shown in Equation (18):

$$\begin{cases} \lambda_j = 1 \to |00\rangle \\ \lambda_j = -i \to |01\rangle \\ \lambda_j = -1 \to |10\rangle \\ \lambda_j = i \to |11\rangle \end{cases}. \quad (18)$$

We know that the eigenvector $|u\rangle$ can be written in standard orthogonal basis form, as shown in Equation (19):

$$|u\rangle = \sum_j b_j |u_j\rangle, \quad (19)$$

where b_j is the projection length. Thus, Equation (8) can also be written as:

$$|\psi_3\rangle = \sum_j |\phi_j\rangle b_j |u_j\rangle, \tag{20}$$

where $|\phi_j\rangle \in \{|00\rangle, |01\rangle, |10\rangle, |11\rangle\}$; $j = 0, 1, \cdots, n-1$. Next, the phase gates $R_Z(-\pi\alpha)$ and $R_Z(-\pi\alpha/2)$ are expressed as:

$$R_Z(-\pi\alpha) = \begin{pmatrix} 1 & 0 \\ 0 & e^{-\pi i\alpha} \end{pmatrix} \tag{21}$$

and

$$R_Z(-\pi\alpha/2) = \begin{pmatrix} 1 & 0 \\ 0 & e^{-\pi i\alpha/2} \end{pmatrix}. \tag{22}$$

We can obtain the quantum state $|\psi_4\rangle$ by

$$|\psi_4\rangle = \sum_j e^{-\pi i\alpha\phi_j/2} |\phi_j\rangle \otimes b_j |u_j\rangle. \tag{23}$$

The 2-qubit *QFT* can be expressed as:

$$QFT = \frac{1}{\sqrt{4}} \begin{pmatrix} 1 & 1 & 1 & 1 \\ 1 & -i & -1 & i \\ 1 & -1 & 1 & -1 \\ 1 & i & -1 & -i \end{pmatrix}. \tag{24}$$

After the *QFT* of $|\phi_j\rangle$, the eigenvalues are restored:

$$\begin{aligned} |\psi_5\rangle &= \frac{1}{2}\left(\sum_j e^{-\pi i\alpha\phi_j/2} \lambda_j^0 b_j |u_j\rangle |00\rangle + \sum_j e^{-\pi i\alpha\phi_j/2} \lambda_j^1 b_j |u_j\rangle |01\rangle + \sum_j e^{-\pi i\alpha\phi_j/2} \lambda_j^2 b_j |u_j\rangle |10\rangle + \sum_j e^{-\pi i\alpha\phi_j/2} \lambda_j^3 b_j |u_j\rangle |11\rangle \right) \\ &= \frac{1}{2}\left(\sum_j e^{-\pi i\alpha\phi_j/2} b_j |u_j\rangle |00\rangle + \sum_j e^{-\pi i\alpha\phi_j/2} F b_j |u_j\rangle |01\rangle + \sum_j e^{-\pi i\alpha\phi_j/2} F^2 b_j |u_j\rangle |10\rangle + \sum_j e^{-\pi i\alpha\phi_j/2} F^3 b_j |u_j\rangle |11\rangle \right) \end{aligned}, \tag{25}$$

where $\phi_j \in \{0, 1, 2, 3\}$. Then,

$$\begin{aligned} |\psi_6\rangle &= \frac{1}{2}\left(\sum_j e^{-\pi i\alpha\phi_j/2} \lambda_j^0 b_j |u_j\rangle |00\rangle + \sum_j e^{-\pi i\alpha\phi_j/2} IFF b_j |u_j\rangle |01\rangle + \sum_j e^{-\pi i\alpha\phi_j/2} IF^2 F^2 b_j |u_j\rangle |10\rangle + \sum_j e^{-\pi i\alpha\phi_j/2} IF^3 F^3 b_j |u_j\rangle |11\rangle \right) \\ &= \frac{1}{2}\left(\sum_j e^{-\pi i\alpha\phi_j/2} b_j |u_j\rangle |00\rangle + \sum_j e^{-\pi i\alpha\phi_j/2} b_j |u_j\rangle |01\rangle + \sum_j e^{-\pi i\alpha\phi_j/2} b_j |u_j\rangle |10\rangle + \sum_j e^{-\pi i\alpha\phi_j/2} b_j |u_j\rangle |11\rangle \right) \\ &= \sum_j e^{-\pi i\alpha\phi_j/2} b_j |u_j\rangle \frac{1}{\sqrt{2}}(|0\rangle + |1\rangle) \frac{1}{\sqrt{2}}(|0\rangle + |1\rangle) \end{aligned}, \tag{26}$$

where *IF* denotes the inverse Fourier transform. Finally, through the *H* gate, we obtain $|\psi_7\rangle$:

$$|\psi_7\rangle = |0\rangle|0\rangle \sum_j e^{-\pi i\alpha\phi_j/2} b_j |u_j\rangle. \tag{27}$$

From Equations (1) and (2), we know that

$$\sum_j e^{-\pi i\phi_j/2} b_j |u_j\rangle = F|u\rangle, \tag{28}$$

$$\sum_j e^{-\pi i\alpha\phi_j/2} b_j |u_j\rangle = F^\alpha |u\rangle. \tag{29}$$

Then, Equation (27) can be expressed as:

$$|\psi_7\rangle = |0\rangle|0\rangle F^\alpha |u\rangle. \tag{30}$$

Therefore, the *QFrFT* is obtained.

In Figure 2, the upper half is the control register, and the lower half is the target register. As the eigenvalues of *QFT* are only 4, the scale of the *QFT* and *IQFT* in the control register is 2-qubit, while the scale of the *QFT* and *IQFT* in the target register can be arbitrary. The *QFrFT* uses two additional auxiliary qubits (i.e., control registers) in space. In time, when the target register is large, only the quantum gate complexity is considered. The complexity of the *QFT* is $O(n^2)$, where n is the number of qubits of the target register [1].

3. Classical Algorithm Corresponding to the *QFrFT*

There exist diverse definitions for the *DFrFT* [29]. This section analyses the correspondence between the proposed *QFrFT* and classical algorithms. The design idea underlying the proposed *QFrFT* is the fractional power of the eigenvalues. We know that the *DFT* can be expressed as eigenvalues and eigenvectors, as shown in Equation (31):

$$F = VDV^T, \tag{31}$$

where D is the eigenvalue matrix and $V = [v_0|v_1|\cdots v_{N-2}|v_{N-1}\ ]$ is the eigenvector. Thus, the *DFrFT* can be expressed as:

$$F^\alpha = VD^\alpha V^T. \tag{32}$$

The eigenvalues of the *FT* are 1, i, -1, and $-i$. Therefore, Equations (31) and (32) can be further expressed as:

$$F = \sum_{k\in E_1}(1)v_k v_k^T + \sum_{k\in E_2}(-i)v_k v_k^T + \sum_{k\in E_3}(-1)v_k v_k^T + \sum_{k\in E_4}(i)v_k v_k^T \tag{33}$$

and

$$F^\alpha = \sum_{k\in E_1}(1)^\alpha v_k v_k^T + \sum_{k\in E_2}(-i)^\alpha v_k v_k^T + \sum_{k\in E_3}(-1)^\alpha v_k v_k^T + \sum_{k\in E_4}(i)^\alpha v_k v_k^T, \tag{34}$$

where E_1, E_2, E_3, and E_4 represent the set of subscripts corresponding to the respective eigenvalues and eigenvectors. For the *QFrFT* in Figure 2, the important calculation steps are

$$\begin{aligned} IQFT\big(I|00\rangle + F|01\rangle + F^2|10\rangle + F^3|11\rangle\big) &= IQFT\begin{pmatrix} I \\ F \\ F^2 \\ F^3 \end{pmatrix} \\ &= \frac{1}{\sqrt{4}}\begin{pmatrix} 1 & 1 & 1 & 1 \\ 1 & i & -1 & -i \\ 1 & -1 & 1 & -1 \\ 1 & -i & -1 & i \end{pmatrix}\begin{pmatrix} I \\ F \\ F^2 \\ F^3 \end{pmatrix} \end{aligned}. \tag{35}$$

Let

$$\begin{cases} Y_0 = I + F + F^2 + F^3 \\ Y_1 = I + iF - F^2 - iF^3 \\ Y_2 = I - F + F^2 - F^3 \\ Y_3 = I - iF - F^2 + iF^3 \end{cases}. \tag{36}$$

At this point, we can obtain

$$\begin{cases} Y_0|u\rangle = \big(D^0 + D^1 + D^2 + D^3\big)|u\rangle \\ Y_1|u\rangle = \big(D^0 + iD^1 - D^2 - iD^3\big)|u\rangle \\ Y_2|u\rangle = \big(D^0 - D^1 + D^2 - D^3\big)|u\rangle \\ Y_3|u\rangle = \big(D^0 - iD^1 - D^2 + iD^3\big)|u\rangle \end{cases}. \tag{37}$$

Then,

$$\begin{cases} Y_0|u\rangle = Q|u\rangle \\ Y_1|u\rangle = W|u\rangle \\ Y_2|u\rangle = E|u\rangle \\ Y_3|u\rangle = R|u\rangle \end{cases}. \tag{38}$$

From the above results in Equations (14)–(17) for Q, W, E, and R, Equation (36) can be expressed as:

$$\begin{cases} Y_0 = \sum_{k\in E_1} v_k v_k^T \\ Y_1 = \sum_{k\in E_2} v_k v_k^T \\ Y_2 = \sum_{k\in E_3} v_k v_k^T \\ Y_3 = \sum_{k\in E_4} v_k v_k^T \end{cases}. \tag{39}$$

From the phase gates shown in Figure 2, we can obtain

$$\begin{pmatrix} 1 & 0 \\ 0 & e^{-\pi i\alpha} \end{pmatrix} \otimes \begin{pmatrix} 1 & 0 \\ 0 & e^{-\pi i\alpha/2} \end{pmatrix} = \begin{pmatrix} 1 & & & 0 \\ & e^{-\pi i\alpha/2} & & \\ & & e^{-2\pi i\alpha/2} & \\ 0 & & & e^{-3\pi i\alpha/2} \end{pmatrix} = \begin{pmatrix} (1)^{\alpha} & & & 0 \\ & (-i)^{\alpha} & & \\ & & (-1)^{\alpha} & \\ 0 & & & (i)^{\alpha} \end{pmatrix}. \tag{40}$$

Thus, Equation (34) can be obtained by combining Equations (39) and (40). Thus, the mathematical principle of the *QFrFT* is explained.

Considering the many definitions of the *DFrFT* [29], we found that Shih's *FrFT* is consistent with the proposed *QFrFT*. In 1995, Shih proposed the *FrFT* using the weighted combination of four functions [30]. Its definition can be expressed as:

$$(F^{\alpha} f)(t) = \sum_{l=0}^{3} A_l^{\alpha} f_l(t), \tag{41}$$

where $f_l(t) = F^l[f(t)]; l = 0, 1, 2, 3$. The weighting coefficient A_l^{α} can be further written as:

$$\begin{aligned} A_l^{\alpha} &= \cos\left(\frac{(\alpha-l)\pi}{4}\right)\cos\left(\frac{2(\alpha-l)\pi}{4}\right)\exp\left(-\frac{3(\alpha-l)i\pi}{4}\right) \\ &= \frac{1}{2} \times \left[\exp\left(\frac{(\alpha-l)\pi i}{4}\right) + \exp\left(\frac{-(\alpha-l)\pi i}{4}\right)\right] \\ &\times \frac{1}{2} \times \left[\exp\left(\frac{2(\alpha-l)\pi i}{4}\right) + \exp\left(\frac{-2(\alpha-l)\pi i}{4}\right)\right] \times \exp\left(-\frac{3(\alpha-l)i\pi}{4}\right) \\ &= \frac{1}{4}\left(1 + \exp\left(-\frac{2(\alpha-l)\pi i}{4}\right) + \exp\left(-\frac{4(\alpha-l)\pi i}{4}\right) + \exp\left(-\frac{6(\alpha-l)\pi i}{4}\right)\right) \\ &= \frac{1}{4}\sum_{k=0}^{3} \exp\left(-\frac{2\pi i}{4}(\alpha-l)k\right) \\ &= \frac{1}{4}\sum_{k=0}^{3} \exp\left(-\frac{2\pi i\alpha k}{4}\right)\exp\left(\frac{2\pi ikl}{4}\right) \end{aligned}. \tag{42}$$

Therefore, the weighting coefficient A_l^{α} can be written in matrix form

$$\begin{pmatrix} A_0^{\alpha} \\ A_1^{\alpha} \\ A_2^{\alpha} \\ A_3^{\alpha} \end{pmatrix} = \frac{1}{4}\begin{pmatrix} 1 & 1 & 1 & 1 \\ 1 & i & -1 & -i \\ 1 & -1 & 1 & -1 \\ 1 & -i & -1 & i \end{pmatrix}\begin{pmatrix} B_0^{\alpha} \\ B_1^{\alpha} \\ B_2^{\alpha} \\ B_3^{\alpha} \end{pmatrix}, \tag{43}$$

where $B_k^\alpha = \exp\left(-\frac{2\pi i k\alpha}{4}\right); k = 0,1,2,3$. Thus, Shih's *FrFT* can be expressed as:

$$\begin{aligned} F^\alpha[f(t)] &= \left(I, F, F^2, F^3\right)\begin{pmatrix} A_0^\alpha \\ A_1^\alpha \\ A_2^\alpha \\ A_3^\alpha \end{pmatrix} f(t) \\ &= \tfrac{1}{4}\left(I, F, F^2, F^3\right)\begin{pmatrix} 1 & 1 & 1 & 1 \\ 1 & i & -1 & -i \\ 1 & -1 & 1 & -1 \\ 1 & -i & -1 & i \end{pmatrix}\begin{pmatrix} B_0^\alpha \\ B_1^\alpha \\ B_2^\alpha \\ B_3^\alpha \end{pmatrix} f(t) \end{aligned}. \tag{44}$$

From Equation (36), Shih's *FrFT* can be further expressed as:

$$F^\alpha[f(t)] = \frac{1}{4}(Y_0, Y_1, Y_2, Y_3)\begin{pmatrix} B_0^\alpha \\ B_1^\alpha \\ B_2^\alpha \\ B_3^\alpha \end{pmatrix} f(t), \tag{45}$$

where $B_k^\alpha = \exp\left(-\frac{2\pi i k\alpha}{4}\right); k = 0,1,2,3$ and

$$\begin{pmatrix} B_0^\alpha \\ B_1^\alpha \\ B_2^\alpha \\ B_3^\alpha \end{pmatrix} = \begin{pmatrix} (1)^\alpha \\ (-i)^\alpha \\ (-1)^\alpha \\ (i)^\alpha \end{pmatrix}. \tag{46}$$

Thus, we obtain Equation (34). Therefore, Shih's *FrFT* coincides with the proposed *QFrFT*.

4. Implementation of Quantum Multi-Fractional Fourier Transform

Shih's *FrFT* has many extended definitions [31–34], which are collectively referred to as the multi-fractional Fourier transform (*mFrFT*). Next, we focus on the design of quantum algorithms for the *mFrFT*. The implementation of its quantum algorithm will be of great help in the fields of quantum computing and quantum information security. In 2000, Zhu et al. proposed the definition of the *mFrFT* and applied it to image encryption [31]. This definition can be expressed as:

$$F_M^\alpha[f(t)] = \sum_{l=0}^{M-1} A_l^\alpha f_l(t), \tag{47}$$

where the basic functions are $f_l(t) = F^{4l/M}[f(t)]; l = 0,1,\cdots,M-1$. The weighting coefficient A_l^α can be expressed as:

$$\begin{aligned} A_l^\alpha &= \frac{1}{M}\sum_{k=0}^{M-1} \exp\left[-\frac{2\pi i k(\alpha - l)}{M}\right] \\ &= \frac{1}{M}\sum_{k=0}^{M-1} \exp\left(\frac{2\pi i k l}{M}\right)\exp\left(-\frac{2\pi i \alpha k}{M}\right) \\ &= IDFT\left[e^{(-2\pi i \alpha k/M)}\right]_{k=0,1,2,\cdots\cdots,M-1} \end{aligned}. \tag{48}$$

where *IDFT* is the inverse discrete Fourier transform. Furthermore, the weighting coefficients A_l^α can be expressed in matrix form as:

$$\begin{pmatrix} A_0^\alpha \\ A_1^\alpha \\ \vdots \\ A_{M-1}^\alpha \end{pmatrix} = \frac{1}{M}\begin{pmatrix} w^{0\times 0} & w^{0\times 1} & \cdots & w^{0\times(M-1)} \\ w^{1\times 0} & w^{1\times 1} & \cdots & w^{1\times(M-1)} \\ \vdots & \vdots & \ddots & \vdots \\ w^{(M-1)\times 0} & w^{(M-1)\times 1} & \cdots & w^{(M-1)\times(M-1)} \end{pmatrix}\begin{pmatrix} B_0^\alpha \\ B_1^\alpha \\ \vdots \\ B_{M-1}^\alpha \end{pmatrix}, \tag{49}$$

where $w = \exp(2\pi i/M)$ and $B_k^\alpha = \exp\left(-\frac{2\pi i k\alpha}{M}\right), k = 0, 1, \cdots, M-1$. Therefore, Equation (47) can be expressed as:

$$\begin{aligned} F_M^\alpha[f(t)] &= A_0^\alpha f_0(t) + A_1^\alpha f_1(t) + \cdots + A_{M-1}^\alpha f_{M-1}(t) \\ &= A_0^\alpha F^{\frac{0}{M}}[f(t)] + A_1^\alpha F^{\frac{4}{M}}[f(t)] + \cdots + A_{M-1}^\alpha F^{\frac{4(M-1)}{M}}[f(t)] \\ &= \left(I, F^{\frac{4}{M}}, \cdots, F^{\frac{4(M-1)}{M}}\right)\begin{pmatrix} A_0^\alpha \\ A_1^\alpha \\ \vdots \\ A_{M-1}^\alpha \end{pmatrix} f(t) \end{aligned}, \tag{50}$$

Further, we can obtain

$$F_M^\alpha[f(t)] = \frac{1}{M}\left(I, F^{\frac{4}{M}}, \cdots, F^{\frac{4(M-1)}{M}}\right)\begin{pmatrix} w^{0\times 0} & w^{0\times 1} & \cdots & w^{0\times(M-1)} \\ w^{1\times 0} & w^{1\times 1} & \cdots & w^{1\times(M-1)} \\ \vdots & \vdots & \ddots & \vdots \\ w^{(M-1)\times 0} & w^{(M-1)\times 1} & \cdots & w^{(M-1)\times(M-1)} \end{pmatrix}\begin{pmatrix} B_0^\alpha \\ B_1^\alpha \\ \vdots \\ B_{M-1}^\alpha \end{pmatrix} f(t). \tag{51}$$

Here, let

$$\begin{cases} Y_0 = w^{0\times 0}I + w^{1\times 0}F^{\frac{4}{M}} + \cdots + w^{(M-1)\times 0}F^{\frac{4(M-1)}{M}} \\ Y_1 = w^{0\times 1}I + w^{1\times 1}F^{\frac{4}{M}} + \cdots + w^{(M-1)\times 1}F^{\frac{4(M-1)}{M}} \\ Y_2 = w^{0\times 2}I + w^{1\times 2}F^{\frac{4}{M}} + \cdots + w^{(M-1)\times 2}F^{\frac{4(M-1)}{M}} \\ \quad\vdots \\ Y_{M-1} = w^{0\times(M-1)}I + w^{1\times(M-1)}F^{\frac{4}{M}} + \cdots + w^{(M-1)\times(M-1)}F^{\frac{4(M-1)}{M}} \end{cases}. \tag{52}$$

In this way, the *mFrFT* can also be expressed as Equation (53):

$$\begin{aligned} F_M^\alpha[f(t)] &= \tfrac{1}{M}(Y_0, Y_1, \cdots, Y_{M-1})\begin{pmatrix} B_0^\alpha \\ B_1^\alpha \\ \vdots \\ B_{M-1}^\alpha \end{pmatrix} f(t) \\ &= \tfrac{1}{M}\sum_{k=0}^{M-1} Y_k B_k^\alpha f(t) \end{aligned}, \tag{53}$$

where $B_k^\alpha = \exp\left(-\frac{2\pi i k\alpha}{M}\right); k = 0, 1, \cdots, M-1$. Next, analyzing the results of Equation (52), from Equation (37), we obtain

$$\begin{cases} Y_0|u\rangle = \left(w^{0\times 0}D^0 + w^{1\times 0}D^{\frac{4}{M}} + \cdots + w^{(M-1)\times 0}D^{\frac{4(M-1)}{M}}\right)|u\rangle \\ Y_1|u\rangle = \left(w^{0\times 1}D^0 + w^{1\times 1}D^{\frac{4}{M}} + \cdots + w^{(M-1)\times 1}D^{\frac{4(M-1)}{M}}\right)|u\rangle \\ Y_2|u\rangle = \left(w^{0\times 2}D^0 + w^{1\times 2}D^{\frac{4}{M}} + \cdots + w^{(M-1)\times 2}D^{\frac{4(M-1)}{M}}\right)|u\rangle \\ \quad\vdots \\ Y_{M-1}|u\rangle = \left(w^{0\times(M-1)}D^0 + w^{1\times(M-1)}D^{\frac{4}{M}} + \cdots + w^{(M-1)\times(M-1)}D^{\frac{4(M-1)}{M}}\right)|u\rangle \end{cases}. \tag{54}$$

Let

$$\begin{cases} Q_0 = w^{0\times 0}D^0 + w^{1\times 0}D^{\frac{4}{M}} + \cdots + w^{(M-1)\times 0}D^{\frac{4(M-1)}{M}} \\ Q_1 = w^{0\times 1}D^0 + w^{1\times 1}D^{\frac{4}{M}} + \cdots + w^{(M-1)\times 1}D^{\frac{4(M-1)}{M}} \\ Q_2 = w^{0\times 2}D^0 + w^{1\times 2}D^{\frac{4}{M}} + \cdots + w^{(M-1)\times 2}D^{\frac{4(M-1)}{M}} \\ \quad\vdots \\ Q_{M-1} = w^{0\times (M-1)}D^0 + w^{1\times (M-1)}D^{\frac{4}{M}} + \cdots + w^{(M-1)\times (M-1)}D^{\frac{4(M-1)}{M}} \end{cases}. \tag{55}$$

Then,

$$Q_0 = w^{0\times 0}\lambda_j^0 + w^{1\times 0}\lambda_j^{\frac{4}{M}} + \cdots + w^{(M-1)\times 0}\lambda_j^{\frac{4(M-1)}{M}} = \lambda_j^0 + \lambda_j^{\frac{4}{M}} + \cdots + \lambda_j^{\frac{4(M-1)}{M}}, \tag{56}$$

where $\lambda_j \in (1, i, -1, -i)$. For proof, we set $\lambda_j \in \left(e^{\pi i 0/2}, e^{\pi i 1/2}, e^{\pi i 2/2}, e^{\pi i 3/2}\right)$.

When $\lambda_j = 1$,

$$\lambda_j^0 + \lambda_j^{\frac{4}{M}} + \cdots + \lambda_j^{\frac{4(M-1)}{M}} = M. \tag{57}$$

When $\lambda_j = i$,

$$\begin{aligned} \lambda_j^0 + \lambda_j^{\frac{4}{M}} + \cdots + \lambda_j^{\frac{4(M-1)}{M}} &= 1 + e^{2\pi i 1/M} + e^{2\pi i 2/M} + \cdots + e^{2\pi i (M-1)/M} \\ &= \frac{1-\left(e^{2\pi i/M}\right)^M}{1-e^{2\pi i/M}} \\ &= \frac{1-1}{1-e^{2\pi i/M}} \\ &= 0 \end{aligned}. \tag{58}$$

When $\lambda_j = -1$,

$$\begin{aligned} \lambda_j^0 + \lambda_j^{\frac{4}{M}} + \cdots + \lambda_j^{\frac{4(M-1)}{M}} &= 1 + e^{4\pi i 1/M} + e^{4\pi i 2/M} + \cdots + e^{4\pi i (M-1)/M} \\ &= \frac{1-\left(e^{4\pi i/M}\right)^M}{1-e^{2\pi i/M}} \\ &= \frac{1-1}{1-e^{2\pi i/M}} \\ &= 0 \end{aligned}. \tag{59}$$

When $\lambda_j = -1$,

$$\begin{aligned} \lambda_j^0 + \lambda_j^{\frac{4}{M}} + \cdots + \lambda_j^{\frac{4(M-1)}{M}} &= 1 + e^{6\pi i 1/M} + e^{6\pi i 2/M} + \cdots + e^{6\pi i (M-1)/M} \\ &= \frac{1-\left(e^{6\pi i/M}\right)^M}{1-e^{2\pi i/M}} \\ &= \frac{1-1}{1-e^{2\pi i/M}} \\ &= 0 \end{aligned}. \tag{60}$$

So, we can obtain

$$Q_0 = \begin{cases} M,\ \lambda_j = 1 \\ 0,\ \ \lambda_j = i, -1, -i \end{cases}. \tag{61}$$

Next, we calculate Q_1 as

$$Q_1 = w^{0\times 1}D^0 + w^{1\times 1}D^{\frac{4}{M}} + \cdots + w^{(M-1)\times 1}D^{\frac{4(M-1)}{M}} = \sum_{k=0}^{M-1} e^{2\pi i k/M}\lambda_j^{4k/M}, \tag{62}$$

when $\lambda_j \in \left(e^{\pi i 0/2}, e^{\pi i 1/2}, e^{\pi i 2/2}, e^{\pi i 3/2}\right)$, we have $Q_1 = 0$. Moreover, our calculation shows that, for Equation (55), $Q_2 = Q_3 = \cdots = Q_{M-4} = 0$.

So, we calculate Q_{M-3} as

$$Q_{M-3} = w^{0\times(M-3)}D^{0} + w^{1\times(M-3)}D^{\frac{4}{M}} + \cdots + w^{(M-1)\times(M-3)}D^{\frac{4(M-1)}{M}} = \sum_{k=0}^{M-1} e^{2\pi ik(M-3)/M}\lambda_j^{4k/M}, \tag{63}$$

where $\lambda_j \in \left(e^{\pi i0/2}, e^{\pi i1/2}, e^{\pi i2/2}, e^{\pi i3/2}\right)$. Then, we obtain

$$Q_3 = \sum_{k=0}^{M-1} e^{2\pi ik(M-3)/M}\lambda_j^{4k/M} = \sum_{k=0}^{M-1} e^{(2\pi ikM-6\pi ik+2\pi ikh)/M}, \tag{64}$$

where $h = 0,1,2,3$. For Equation (64), when $h = 3$, the result is non-zero and the eigenvalue is $e^{\pi i3/2} = -i$,

$$Q_{M-3} = \begin{cases} M & \lambda = -i \\ 0 & \lambda = 1, i, -1 \end{cases}. \tag{65}$$

For Q_{M-2},

$$\begin{aligned} Q_{M-2} &= w^{0\times(M-2)}D^{0} + w^{1\times(M-2)}D^{\frac{4}{M}} + \cdots + w^{(M-1)\times(M-2)}D^{\frac{4(M-1)}{M}} \\ &= \sum_{k=0}^{M-1} e^{2\pi ik(M-2)/M}\lambda_j^{4k/M} \\ &= \sum_{k=0}^{M-1} e^{(2\pi ikM-4\pi ik+2\pi ikh)/M} \end{aligned}. \tag{66}$$

For Equation (66), when $h = 2$, the result is non-zero and the eigenvalue is $e^{\pi i2/2} = -1$,

$$Q_{M-2} = \begin{cases} M & \lambda = -1 \\ 0 & \lambda = 1, i, -i \end{cases}. \tag{67}$$

For Q_{M-1},

$$\begin{aligned} Q_{M-1} &= w^{0\times(M-1)}D^{0} + w^{1\times(M-1)}D^{\frac{4}{M}} + \cdots + w^{(M-1)\times(M-1)}D^{\frac{4(M-1)}{M}} \\ &= \sum_{k=0}^{M-1} e^{2\pi ik(M-1)/M}\lambda_j^{4k/M} \\ &= \sum_{k=0}^{M-1} e^{(2\pi ikM-2\pi ik+2\pi ikh)/M} \end{aligned}. \tag{68}$$

For Equation (68), when $h = 1$, the result is non-zero and the eigenvalue is $e^{\pi i/2} = i$,

$$Q_{M-1} = \begin{cases} M & \lambda = i \\ 0 & \lambda = 1, -1, -i \end{cases}. \tag{69}$$

Therefore, for Equation (52), only Y_0, Y_{M-3}, Y_{M-2}, and Y_{M-1} are non-zero, while the other terms are zero. If the eigenvalue $\lambda_j \in \left(e^{-\pi i0/2}, e^{-\pi i1/2}, e^{-\pi i2/2}, e^{-\pi i3/2}\right)$, in Equation (55), only Q_0, Q_1, Q_2, and Q_3 are non-zero, while the other results are zero. For Equation (53), there are only four effective weighting terms for the *mFrFT*.

However, for Equation (53), when B_k^{α} takes different values, we obtain different definitions [35]. For example, $B_k^{\alpha} = \exp\left(-\frac{2\pi ik\alpha}{4}\right)$; $k = 0,1,2,3$ gives Shih's *FrFT* [30]; $B_k^{\alpha} = \exp\left(-\frac{2\pi ik\alpha}{M}\right)$; $k = 0,1,\cdots,M-1$ gives the *mFrFT* of Zhu et al. [31]; $B_k^{\alpha} = \exp\left[-\frac{2\pi i(m_kM+1)\alpha(n_kM+k)}{M}\right]$; $k = 0,1,\cdots,M-1$ gives the multi-parameter fractional Fourier transform of Tao et al. [32]; $B_k^{\alpha} = \exp\left[-\frac{2\pi i\alpha(r_kM+l)}{M}\right]$; $k = 0,1,\cdots,M-1$ gives the modified multi-parameter fractional Fourier transform of Ran et al. [33]; and $B_k^{\overline{\alpha}} = \exp\left[-\frac{2\pi i\alpha_l(r_lM+l)}{M}\right]$; $k = 0,1,\cdots,M-1$ gives the vector power multi-parameter fractional Fourier transform of Ran et al. [34].

Obviously, all of these extended definitions also have only four effective weighting terms, which has a great impact on the application of these algorithms in signal processing and image encryption.

5. Discussion

5.1. Phase Gates

For the *QFrFT* shown in Figure 2, we select the phase gates $R_Z(-\pi\alpha)$ and $R_Z(-\pi\alpha/2)$. If the phase gates $R_Z(\pi\alpha)$ and $R_Z(\pi\alpha/2)$ are selected, the *QFrFT* circuit is as shown in Figure 3.

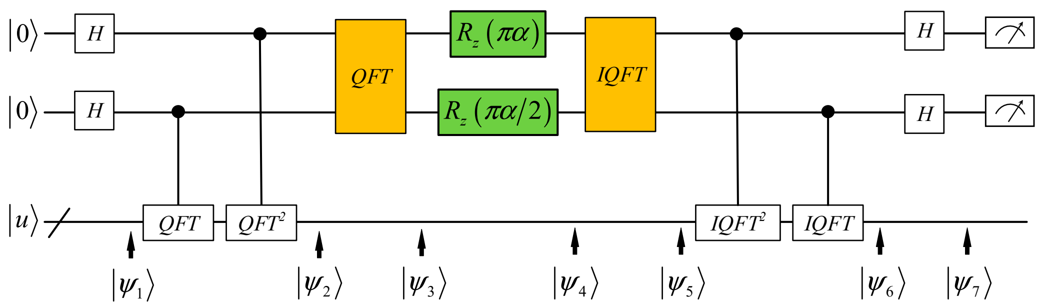

Figure 3. *QFrFT* circuit with both phase gates and *QFT* changed (the colored parts have changed relative to Figure 2).

From Figure 3, we can see that the phase gates have changed, and the order of the *QFT* and the *IQFT* regarding the 2-qubits in the control register has also changed. This is to ensure that the eigenvalues correspond to the eigenvectors. The correspondence between the eigenvalues of the control register is:

$$\begin{cases} \lambda_j = 1 \rightarrow |00\rangle \\ \lambda_j = i \rightarrow |01\rangle \\ \lambda_j = -1 \rightarrow |10\rangle \\ \lambda_j = -i \rightarrow |11\rangle \end{cases}. \tag{70}$$

From the phase gates $R_Z(\pi\alpha)$ and $R_Z(\pi\alpha/2)$, we obtain

$$\begin{pmatrix} 1 & 0 \\ 0 & e^{\pi i\alpha} \end{pmatrix} \otimes \begin{pmatrix} 1 & 0 \\ 0 & e^{\pi i\alpha/2} \end{pmatrix} = \begin{pmatrix} 1 & & & 0 \\ & e^{\pi i\alpha/2} & & \\ & & e^{2\pi i\alpha/2} & \\ 0 & & & e^{3\pi i\alpha/2} \end{pmatrix} = \begin{pmatrix} (1)^{\alpha} & & & 0 \\ & (i)^{\alpha} & & \\ & & (-1)^{\alpha} & \\ 0 & & & (-i)^{\alpha} \end{pmatrix}. \tag{71}$$

This ensures the correspondence between eigenvalues and eigenvectors. Thus, we have

$$F = \sum_{k\in E_1} (1)v_k v_k^T + \sum_{k\in E_2} (i)v_k v_k^T + \sum_{k\in E_3} (-1)v_k v_k^T + \sum_{k\in E_4} (-i)v_k v_k^T \tag{72}$$

and

$$F^{\alpha} = \sum_{k\in E_1} (1)^{\alpha}v_k v_k^T + \sum_{k\in E_2} (i)^{\alpha}v_k v_k^T + \sum_{k\in E_3} (-1)^{\alpha}v_k v_k^T + \sum_{k\in E_4} (-i)^{\alpha}v_k v_k^T. \tag{73}$$

The *QFrFT* and Shih's *FrFT* are the same. To ensure that the eigenvalues correspond to the eigenvectors, when the eigenvalues become fractional powers, they also correspond to the eigenvectors. Therefore, the key idea of the algorithm's design is to retain the eigenvector of the *FT*, such that the eigenvalue takes a fractional power.

Considering Figure 2, if we only change the phase gates, the result is shown in Figure 4. The relevant correspondence between the eigenvalues and eigenvectors is shown in Equations (33) and (73). In this way, the obtained results do not correspond to the feature vector of the *FT* and, so, the design scheme shown in Figure 4 is not feasible.

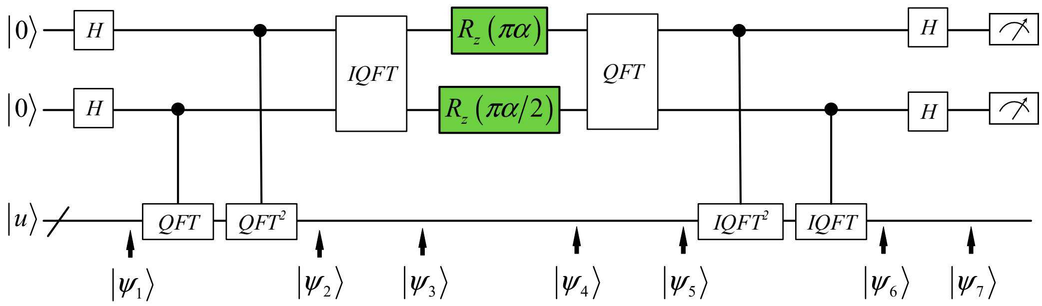

Figure 4. *QFrFT* circuit with only the phase gates changed (the colored parts have changed relative to Figure 2).

5.2. Flaws of the mFrFT

From the design of the quantum *mFrFT*, we find that there are many invalid weighting terms in the definition of classical *mFrFT*. The reason for this problem is due to the eigenvalues of the algorithm. We know that the eigenvalues of the *FT* are 1, i, -1 and $-i$, and the time–frequency spatial distribution is shown in Figure 5. For Equation (54), the sum of eigenvalues can be expressed as a change in angle in Figure 5.

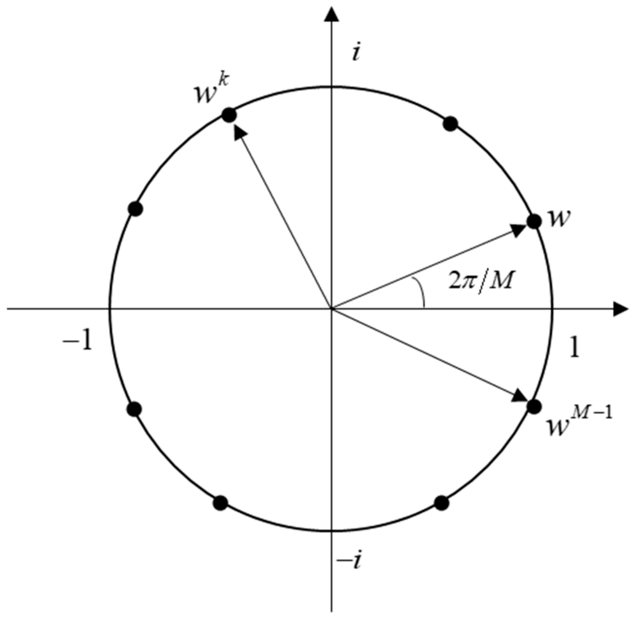

Figure 5. Time–frequency distribution of eigenvalues.

For angle θ, we set

$$w = e^{i\theta}, \tag{74}$$

where $\theta = 2\pi/M$. We can obtain

$$1 + w + w^2 + \cdots + w^{M-1} = 0. \tag{75}$$

Furthermore, we have

$$1 + w^h + w^{2h} + \cdots + w^{(M-1)h} = \begin{cases} M & h = 0 \\ 0 & h \neq 0 \end{cases}. \tag{76}$$

Thus, Equation (64) can be expressed as

$$\sum_{k=0}^{M-1} e^{(2\pi ikM - 6\pi ik + 2\pi ikh)/M} = \sum_{k=0}^{M-1} e^{2\pi ik} e^{\frac{2\pi ik}{M}(h-3)}. \tag{77}$$

Here, $e^{2\pi ik} = 1$. Therefore, the result of Equation (77) is non-zero only when $h = 3$. The other results are also confirmed.

Since 2000, Zhu's *mFrFT* [31] and previous results [36], as well as some extended definitions, have been shown to have flaws [32–34], which we discussed in terms of the eigenvalues of the *QFT*. In the extended definition, the number of effective weighting terms depends on the period of the matrix; for example, the period of the *FT* matrix is 4, so its effective weighting is 4, while the period of the Hadamard transform is 2, so the effective weighting term is defined as 2 accordingly.

6. Conclusions

In this paper, we used the *QFT* and *QPE* to design the *QFrFT*. We retained the eigenvectors of the *QFT* and forced its eigenvalues to take fractional powers. As diverse definitions for the *DFrFT* exist, we determined the correspondence between the proposed *QFrFT* and classical algorithms, which lays the foundation for future application of the *QFrFT* to solve practical problems. Regarding the design of the quantum *mFrFT*, we observed a flaw in the definition of classical algorithms—namely, there are only four effective weighting terms in a series of *mFrFT* definitions—which has a significant impact on the applicability of the algorithms. Finally, we discussed the correspondence between eigenvalues and eigenvectors in the *QFrFT* circuit and analyzed the definition of the algorithm in depth. Furthermore, the defects of the *mFrFT* were mathematically explained.

Author Contributions: Methodology, T.Z.; validation, T.Z. and Y.C.; investigation, T.Z.; writing—original draft preparation, T.Z.; writing—review and editing, T.Z.; supervision, T.Z.; project administration, T.Z.; funding acquisition, T.Z. All authors have read and agreed to the published version of the manuscript.

Funding: This study was supported by the Fundamental Research Funds for the Central Universities (N2123016); and the Scientific Research Projects of Hebei colleges and universities (QN2020511).

Data Availability Statement: Not applicable.

Conflicts of Interest: The authors declare no conflict of interest.

References

1. Nielsen, M.A.; Chuang, I.L. Quantum computation and quantum information. *Phys. Today* **2001**, *54*, 60.
2. Feynman, R.P. Simulating physics with computers. *Int. J. Theor. Phys.* **1982**, *21*, 467–488. [CrossRef]
3. Shor, P.W. Algorithms for Quantum Computation: Discrete Logarithms and Factoring. In Proceedings of the 35th Annual Symposium on Foundation of Computer Science, Washington, DC, USA, 20–22 November 1994; pp. 124–134.
4. Coppersmith, D. An approximate Fourier transform useful in quantum factoring. *arXiv* **2002**. [CrossRef]
5. Flamini, F.; Spagnolo, N.; Sciarrino, F. Photonic quantum information processing: A review. *Rep. Prog. Phys.* **2018**, *82*, 016001. [PubMed]
6. Biamonte, J.; Wittek, P.; Pancotti, N.; Rebentrost, P.; Wiebe, N.; Lloyd, S. Quantum machine learning. *Nature* **2017**, *549*, 195–202.
7. Beer, K.; Bondarenko, D.; Farrelly, T.; Osborne, T.J.; Salzmann, R.; Scheiermann, D.; Wolf, R. Training deep quantum neural networks. *Nat. Commun.* **2020**, *11*, 808. [CrossRef]
8. Venegas-Andraca, S.E.; Bose, S. Quantum computation and image processing: New trends in artificial intelligence. In Proceedings of the IJCAI, Acapulco, Mexico, 9–15 August 2003.
9. Latorre, J.I. Image compression and entanglement. *arXiv* **2005**. [CrossRef]
10. Venegas-Andraca, S.E.; Ball, J. Processing images in entangled quantum systems. *Quantum Inf. Process.* **2010**, *9*, 1–11. [CrossRef]
11. Le, P.Q.; Iliyasu, A.M.; Dong, F.; Hirota, K. A flexible representation and invertible transformations for images on quantum computers. In *New Advances in Intelligent Signal Processing. Studies in Computational Intelligence*; Ruano, A.E., Várkonyi-Kóczy, A.R., Eds.; Springer: Berlin/Heidelberg, Germany, 2011; Volume 372, pp. 179–202.
12. Zhang, Y.; Lu, K.; Gao, Y.; Wang, M. NEQR: A novel enhanced quantum representation of digital images. *Quantum Inf. Process.* **2013**, *12*, 2833–2860. [CrossRef]
13. Wang, Z.; Xu, M.; Zhang, Y. Review of quantum image processing. *Arch. Comput. Methods Eng.* **2022**, *29*, 737–761.
14. Zhang, Y.; Lu, K.; Xu, K.; Gao, Y.; Wilson, R. Local feature point extraction for quantum images. *Quantum Inf. Process.* **2015**, *14*, 1573–1588. [CrossRef]
15. Li, P.; Liu, X.; Xiao, H. Quantum image weighted average filtering in spatial domain. *Int. J. Theor. Phys.* **2017**, *56*, 3690–3716. [CrossRef]

16. Liu, K.; Zhang, Y.; Lu, K.; Wang, X. Restoration for noise removal in quantum images. *Int. J. Theor. Phys.* **2017**, *56*, 2867–2886. [CrossRef]
17. Yin, H.; Lu, D.; Zhang, R. Quantum Windowed Fourier Transform and its Application to Quantum Signal Processing. *Int. J. Theor. Phys.* **2021**, *60*, 3896–3918. [CrossRef]
18. Asaka, R.; Sakai, K.; Yahagi, R. Quantum circuit for the fast Fourier transform. *Quantum Inf. Process.* **2020**, *19*, 277. [CrossRef]
19. Ruiz-Perez, L.; Garcia-Escartin, J.C. Quantum arithmetic with the quantum Fourier transform. *Quantum Inf. Process.* **2017**, *16*, 152. [CrossRef]
20. Lohmann, A.W. Image rotation, Wigner rotation, and the fractional Fourier transform. *JOSA A* **1993**, *10*, 2181–2186. [CrossRef]
21. Bernardo, L.M.; Soares, O.D. Fractional Fourier transforms and optical systems. *Opt. Commun.* **1994**, *110*, 517–522. [CrossRef]
22. Hennelly, B.M.; Sheridan, J.T. Image encryption and the fractional Fourier transform. *Optik* **2003**, *114*, 251–265. [CrossRef]
23. Sejdić, E.; Djurović, I.; Stanković, L. Fractional Fourier transform as a signal processing tool: An overview of recent developments. *Signal Process.* **2011**, *91*, 1351–1369.
24. Gaglione, D.; Clemente, C.; Ilioudis, C.V.; Persico, A.R.; Proudler, I.K.; Soraghan, J.J.; Farina, A. Waveform design for communicating radar systems using fractional Fourier transform. *Digit. Signal Process.* **2018**, *80*, 57–69. [CrossRef]
25. Parasa, V.; Perkowski, M. In Quantum pseudo-fractional fourier transform using multiple-valued logic. In Proceedings of the 2012 IEEE 42nd International Symposium on Multiple-Valued Logic, Victoria, BC, Canada, 14–16 May 2012; pp. 311–314.
26. Lv, C.-H.; Fan, H.-Y.; Li, D.-W. From fractional Fourier transformation to quantum mechanical fractional squeezing transformation. *Chin. Phys. B* **2015**, *24*, 020301. [CrossRef]
27. Weimann, S.; Perez-Leija, A.; Lebugle, M.; Keil, R.; Tichy, M.; Gräfe, M.; Heilmann, R.; Nolte, S.; Moya-Cessa, H.; Weihs, G. Implementation of quantum and classical discrete fractional Fourier transforms. *Nat. Commun.* **2016**, *7*, 11027. [CrossRef] [PubMed]
28. Madrid, Y.; Molina, M.; Torres, R. Quantum Fractional Fourier Transform. In *Frontiers in Optics*; Optica Publishing Group: Washington, DC, USA, 2018.
29. Gómez-Echavarría, A.; Ugarte, J.P.; Tobón, C. The fractional Fourier transform as a biomedical signal and image processing tool: A review. *Biocybern. Biomed. Eng.* **2020**, *40*, 1081–1093.
30. Shih, C.-C. Fractionalization of Fourier transform. *Opt. Commun.* **1995**, *118*, 495–498. [CrossRef]
31. Zhu, B.; Liu, S.; Ran, Q. Optical image encryption based on multifractional Fourier transforms. *Opt. Lett.* **2000**, *25*, 1159–1161. [CrossRef]
32. Tao, R.; Lang, J.; Wang, Y. Optical image encryption based on the multiple-parameter fractional Fourier transform. *Opt. Lett.* **2008**, *33*, 581–583. [CrossRef]
33. Ran, Q.; Zhang, H.; Zhang, J.; Tan, L.; Ma, J. Deficiencies of the cryptography based on multiple-parameter fractional Fourier transform. *Opt. Lett.* **2009**, *34*, 1729–1731. [CrossRef]
34. Ran, Q.; Zhao, T.; Yuan, L.; Wang, J.; Xu, L. Vector power multiple-parameter fractional Fourier transform of image encryption algorithm. *Opt. Laser Eng.* **2014**, *62*, 80–86. [CrossRef]
35. Zhao, T.; Ran, Q. The weighted fractional Fourier transform and its application in image encryption. *Math. Probl. Eng.* **2019**, *2019*, 4789194. [CrossRef]
36. Liu, S.; Jiang, J.; Zhang, Y.; Zhang, J. Generalized fractional Fourier transforms. *J. Phys. A Math. Gen.* **1997**, *30*, 973. [CrossRef]